



ORIGINAL ARTICLE

Open Access



Energetics of the distribution of cell wall in wood based on an eigenvalue analysis

Harusa Tsutsumi^{1,2}, Hirokazu Haga² and Takaaki Fujimoto^{2*}

Abstract

Wood is a highly heterogeneous material characterized by a number of properties that vary significantly among samples. Even in woods of the same density, substantial differences in properties show up depending on the distribution pattern of their cell walls. With the aim of deep understanding of the wood variation, we examine this pattern from the physical perspectives using samples of the same density but with significantly different shrinkages. The power spectrum, which represents the regularity of the occurrence of cell walls or lumen, was obtained through Fourier transform processing of micrographs of the transverse sections of wood samples. The set of eigenvalues calculated from the variance–covariance matrix comprising the spectra is identified with a Hamiltonian representing the energy eigenstate of the wood. The cell wall distribution can then be analyzed from within thermodynamics and statistical mechanics. The eigenvalues from the images of latewood were widely distributed compared with those from earlywood. The first eigenvalue is equivalent to the Helmholtz free energy, and thus the high-shrinkage samples showed large Helmholtz free energy because of the high presence of latewood. The Shannon entropy calculated from the probability associated with each energy eigenstate was larger in images of earlywood than latewood. That is, low-shrinkage samples have a more homogeneous structure than high-shrinkage samples. These results were strongly consistent with observations from micrographs and previous knowledge of the physical properties of woods. The physical approaches proposed in this study is independent of the origin of the data and therefore has a wide application.

Keywords: Fourier spectrum, Random matrix, Information statistical physics, Helmholtz free energy, Entropy

Introduction

Microscope observations of wood show that for each wood species cells of various sizes and shapes are arranged in identifiable patterns [1, 2]. The differences in cell arrangements can be identified from the distribution of the cell walls. The pattern of its distribution determines the characteristics of the wood species. If the cell wall is densely packed, wood density simply increases and strength and dimensional changes increase as a result [3]. Moreover, woods of almost the same density show substantially differences in stiffness and shrinkage [4, 5]. We must be able to evaluate quantitatively not only the amount of cell walls but also their distribution patterns.

The Fourier transform analysis of images introduced by Fujita and coworkers is a noteworthy method for assessing the cell-wall distribution quantitatively [6, 7]. From the power spectrum that is outputted in the fast Fourier transform processing of the dot map of the cell centers, they evaluated the cell arrangements and reconstructed the cell shapes for various wood species [8–15]. Fundamentally, let $\{e_1, e_2, \dots, e_n\}$ be an orthonormal basis for a vector space V of finite dimensions, where n is a positive integer. Then every f in V is uniquely a linear combination $f = \sum f^i e_i$ with f^i an element of a real number space \mathbf{R} . Let $F^i : V \rightarrow \mathbf{R}$ be the linear function that picks out the i th coordinate, $F^i(f) = f^i$; that is, F^i is characterized by

$$F^i(e_j) = \delta_j^i = \begin{cases} 1 & \text{if } i = j; \\ 0 & \text{if } i \neq j. \end{cases} \quad (1)$$

*Correspondence: tafujimoto@tottori-u.ac.jp

² Faculty of Agriculture, Tottori University, Tottori 680-8553, Japan
Full list of author information is available at the end of the article

The coordinate functions F^1, F^2, \dots, F^n then form a basis for the dual space of V , denoted V^* [16]. The Fourier coefficients are simply the coordinate functions and therefore a two-dimensional image data can be identified with a point on \mathbf{R}^n , denoted (f^1, f^2, \dots, f^n) . This perspective plays an important role in the following discussion.

A given wood can be characterized not only by the anatomical features but by many other properties, such as wood density, mechanical properties, and chemical components. In other words, a wood can be defined as a point in \mathbf{R}^n , an n -tuple of numbers $X = (x^1, x^2, \dots, x^n)$. Because wood properties are more or less interrelated, we should evaluate inclusively how multiple characteristics change in relation to the others. Fujimoto suggested a comprehensive method based on the distribution of eigenvalues to evaluate the variation of multiple wood characteristics [4, 5]. In this method, the n -dimensional data obtained from a wood sample is regarded as a state vector representing the physical aspects of the system. Given the advances of measurement technology, the multi-dimensional data of woods can be easily measured for instance from their electromagnetic spectra [17–19]. Although the data variables do not exhibit a one-to-one correspondence with the wood properties, a number of studies have demonstrated that such indirect information can provide the basis for an evaluation of various properties of wood [20–22]. The statistical model obtained in these studies can be regarded as a covector, that is, a mapping from V to \mathbf{R} ($\omega: V \rightarrow \mathbf{R}$) [16]. The set of all covectors on V forms a dual space V^* , which has no essential difference except for the basis. The indirect information can be used to evaluate the actual variations in wood properties comprehensively if they exhibit this dual relationship.

In the context of physics [23, 24], the set of eigenvalues from the data matrix can be identified with the energy of the system and subsequently wood variations can be also analyzed from the perspective of thermodynamics and statistical mechanics [25, 26]. Energy is the one of the most important physical quantities as it appears as a conserved quantity in a wide range of physical systems from thermodynamics to field quantum theory [27]. The evaluation of wood variations based on energy, that is, stochastic energetics [28], would give a completely new perspective on wood science.

We examined the variation in shrinkage using the set of eigenvalues calculated from the near-infrared (NIR) spectral matrix [5]. As discussed later, woods having almost the same density often show substantially different behaviors in shrinkage despite the interaction with water occurring only at the cell wall. The variation in shrinkage is mainly affected by two factors: the distribution pattern of (i) the cell walls in wood and (ii)

the molecular structures in the cell wall [1, 3, 29]. The previous study revealed that the second factor is well explained by the eigenvalues of the NIR spectral matrix [5]. In the current study, the first factor, specifically, that which concerns the effects of the distribution of cell wall on shrinkage, was examined in an eigenvalue analysis. The spectrum obtained from the Fourier transformation of a microscopic image from a cross section of wood was used as the multi-dimensional data. We ensured that this method is independent of the sources of the multi-dimensional data.

Experimental

Materials and shrinkage tests

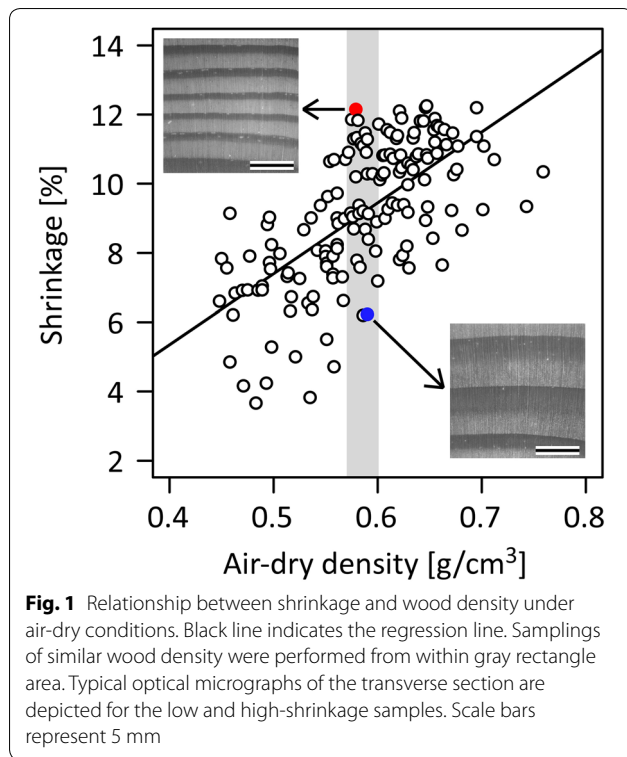
Sample materials were obtained from 50-year-old Japanese larch (*Larix kaempferi*) stands in Tottori University Forest located in Maniwa, Okayama. Detailed information about the origin and processing procedures of the sample was described in our previous article [5]. In brief, a total of 155 samples of dimensions of 20 mm \times 20 mm \times 20 mm were cut from 20 trees and were used in measuring dimensional changes. The specific characteristics of the dimensional changes evaluated were the tangential shrinkage of samples under green to oven-dry conditions, because results obtained from the following analyses were similar in any structural direction of wood. All testing procedures employed conform with the standards set in JIS-Z-2101:1994 [30]. Wood densities were measured under green, air-dry, and oven-dry conditions.

The scatter plot depicting the relationship between shrinkage and wood density under an air-dry condition (Fig. 1) shows a positive linear correlation, albeit very weak (correlation coefficient = 0.69). About twice the difference was found even in samples having similar wood densities (0.585 ± 0.015 g/cm³, gray rectangle area). Twenty samples with similar wood density were then divided into two groups; the first was the low shrinkage group, ranging from 6.20 to 8.90% (mean 7.77%), and the other was the high shrinkage group, ranging from 11.10 to 12.15% (mean 11.52%). Both groups had ten samples.

From the optical micrographs of the transverse section, the transition from earlywood to latewood gradually changed for the low-shrinkage samples; the high-shrinkage samples showed a narrow ring width and a distinct transition from earlywood to latewood. Obvious differences seen in the distribution pattern of cell walls were examined quantitatively and are described next.

Image analysis

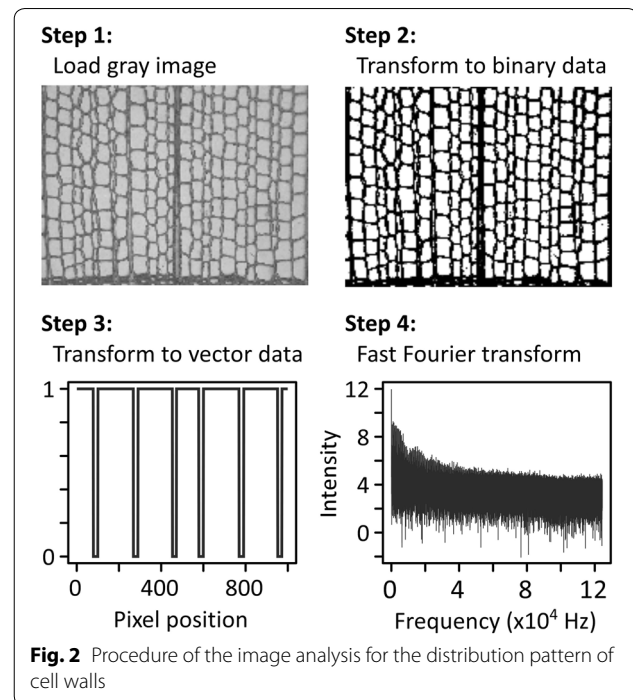
Transverse sections, 20 μ m thick, were cut from one representative sample in both low and high-shrinkage groups using a sliding microtome. The sections were stained in



aqueous safranin and mounted permanently. Image data were captured using a digital camera with a light microscope attached. Consecutive images with field-of-view sizes of $0.5 (T) \times 0.4 (R)$ mm (2560×1920 pixels) were collected for four radial rows and a total of 100 images per section were obtained. The procedures employed in the image analysis (see Fig. 2) involved loading each image into a computer and applying a histogram-based grayscale binarization (Steps 1 and 2). Then, the matrix data of the binarized image was transformed to a vector data (Step 3). A rectangle-pulse signal modeling a Poisson process was chosen to represent the regularity of the cell wall or lumen. To reduce the computation time, the vector transformation was conducted over a limited area of 500×500 pixels located in the center of the image. The length of this vector is then 250,000. Finally, the power spectral density was estimated from the spectrum computed using the fast Fourier transform (Step 4). Image acquisition and data processing were performed using the ‘imager’ [31] and the ‘tuneR’ [32] packages in R ver. 3.3.2.

Eigenvalue analysis

The data analysis procedure is the same as that given in our previous reports [4, 5] except for the origin of the spectrum. With the 100 images obtained per section, we conducted an eigenvalue analysis using matrix data



comprising the 100 power spectra. In brief, an eigenvalue decomposition was applied to the variance–covariance matrix C calculated from the spectral matrix A ($C=A^T A$). The eigenvalue problem is solved by maximizing the quadratic form $\mathbf{u}_i^T C \mathbf{u}_i$ with respect to eigenvector \mathbf{u}_i ($i=1, \dots, N$) [23, 24]. The set of eigenvalues $\{E_1, E_2, \dots, E_N\}$ is regarded as belonging to an energy function, termed the Hamiltonian H . Once H is defined, a distribution function Z can be calculated:

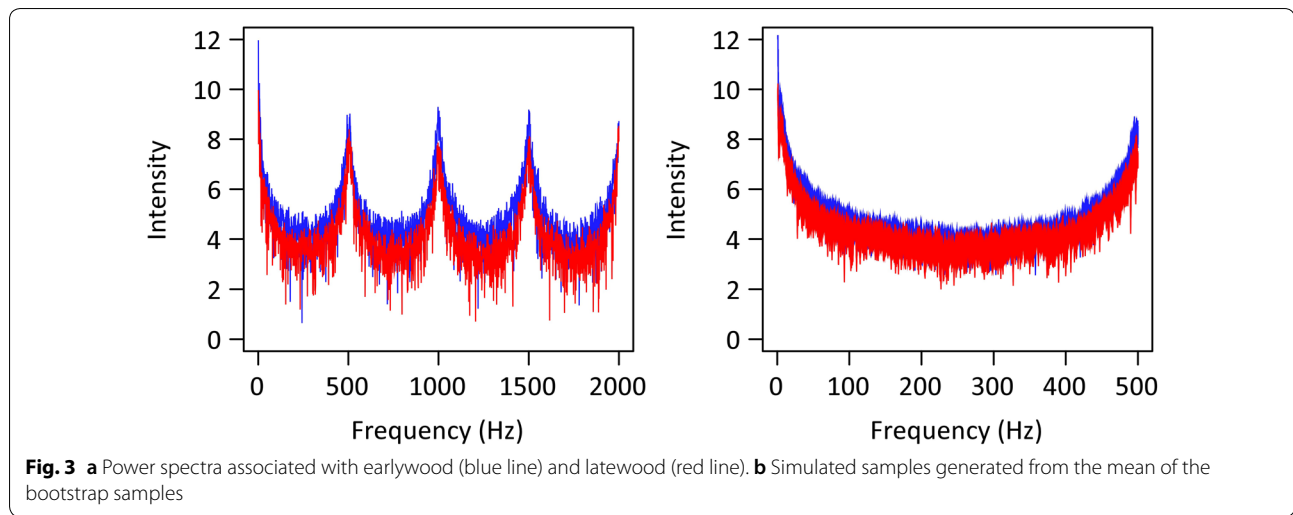
$$Z = \sum_{i=1}^N \exp(-\beta E_i), \quad (2)$$

where β is called the inverse temperature. Thermodynamic functions such as the Helmholtz free energy and entropy can be obtained from the distribution function. With these thermodynamic functions, we compared the distribution patterns of the cell wall for the low and high-shrinkage wood groups.

Results and discussion

Spectral variation

Figure 3a depicts an example of typical power spectra, an enlargement of which is shown in Fig. 2; the blue and red lines indicate the spectra from earlywood and latewood, respectively. The intensities in the spectrum of the earlywood are slightly higher than those for latewood. Both spectra repeat every 500 Hz, probably because of the transformation from matrix to vector.



For this reason, the following analyses are focused on the restricted frequency interval from 1 to 500 Hz with the aim to reduce the computational complexity. In normal spectrum analysis, the peak intensity of a specific frequency is often of most interest. In this study, however, we examined the spectral variations using statistical mechanics and therefore do not consider the spectral variation as individual variables (that is, frequency) separately but rather as a whole for the wood system. Statistical mechanics deals with physical properties of systems that comprise an enormous number of microscopic elements, that is, many-body systems [33–35]. Here, we consider the spectral variables abstractly as microscopic elements comprising the wood system.

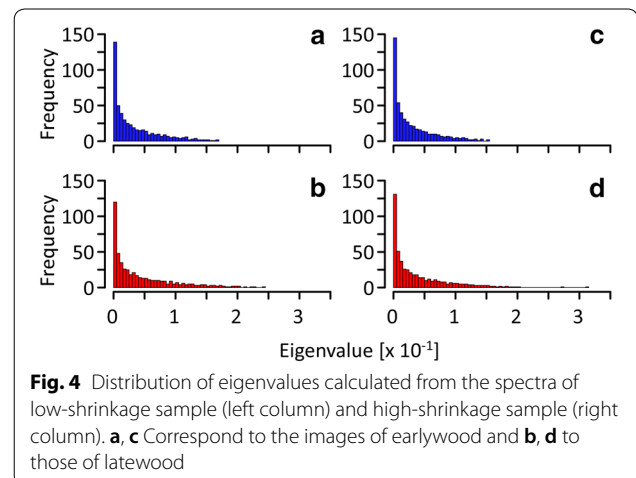
Additionally, we assumed the physical system to be in an equilibrium state that conforms to the requirements of equilibrium statistical physics. In this study, the power spectrum is regarded as a state vector representing the physical state of a given wood. To attain the equilibrium state, many spectra that show an almost similar pattern in variation are required. Prior to the eigenvalue analyses, 500 samples were simulated in accordance with the bootstrap resampling procedure [36]. The intensity at each frequency is assumed to follow an empirical distribution of the measured data, and the mean of the bootstrap samples was obtained by repeating the procedure 500 times using the ‘simpleboot’ package [37]. Simulations were performed with the images of earlywood and latewood. Consequently, spectral matrices corresponding to the earlywood and latewood data, each with 500 rows and 500 columns, were obtained for both low and high-shrinkage samples (Fig. 3b) and were used for the following analyses. The elements of the variance–covariance matrix calculated

from this 500×500 random matrices were assumed to obey a Gaussian orthogonal ensemble [24].

Eigenvalue distribution

From the distributions of the (energy) eigenvalues calculated from the variance–covariance matrix C for low-shrinkage sample (Fig. 4), the eigenvalues from latewood images (panel (b)) are widely distributed compared with those from earlywood images (panel (a)). The same results were found for high-shrinkage sample (Fig. 4c, d). These results indicate that the spectral matrix of the latewood images varied in a more orderly manner than that of the earlywood images. Indeed, the images of latewood were mostly occupied by cell walls and therefore there is no distinctive variation in the distribution of the cell wall.

Using the distribution function Z (Eq. 2) as a normalization factor, the probability that the system of interest is in the energy eigenstate E_i was found to be



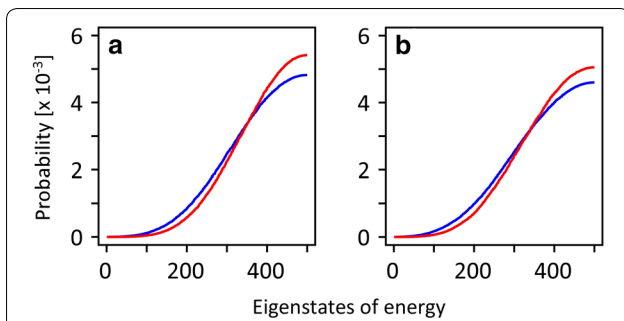


Fig. 5 Probability distributions corresponding to each energy eigenstate calculated from the spectra of low-shrinkage sample (a) and high-shrinkage sample (b). Blue and red lines indicate earlywood and latewood images, respectively

$$p_i = \frac{1}{Z} \exp(-\beta E_i), (i = 1, \dots, N). \tag{3}$$

Let β be a constant. The distribution of probability p_i corresponding to each energy eigenstate (Fig. 5) show that for low (panel (a)) and high (panel (b)) shrinkage samples, p_i of earlywood images (blue lines) has a flat distribution compared with that of latewood images (red lines). This suggests that earlywood displays a more disordered pattern of cell wall distribution compared with latewood. As evident from the optical micrographs (Fig. 1), the low-shrinkage samples contain more earlywood area than the high-shrinkage samples; moreover, the former have a more disordered cellular structure than the latter.

Stochastic energetics for the distribution of cell wall

The thermodynamic functions were calculated using the set of eigenvalues $\{E_1, E_2, \dots, E_N\}$ to assess the distribution pattern of cell wall quantitatively. The Helmholtz free energy F is given by the logarithm of the distribution function,

$$F = \frac{1}{\beta} \log Z. \tag{4}$$

The Helmholtz free energy is an important quantity in the sense that it contains all the information of the physical properties of a system. Although both Z and F depend on β , the first eigenvalue E_1 of the matrix C can be evaluated from F in the limit $\beta \rightarrow \infty$ [23],

$$E_1 = 2 \lim_{\beta \rightarrow \infty} F(\beta|C). \tag{5}$$

As evident in the eigenvalue distribution (Fig. 4), for low and high-shrinkage samples, the first eigenvalues, that is, Helmholtz free energy, associated with the latewood images were higher than those of the earlywood images. The high-shrinkage sample moreover featured a

large Helmholtz free energy because of the high possession of latewood. This result is associated with the distribution pattern of cell walls evident in Fig. 1 and was consistent with our previous understanding that tangential shrinkage and swelling are largely controlled by the changes in the latewood [1]. Because large dimensional changes seem to involve a lot of work arising from the stress during shrinkage or swelling, the result is also consistent with the actual physical picture. This study dealt with woods having almost the same wood density. Hence, the eigenvalues would carry a lot of information concerning various factors other than wood density that influence shrinkage and provide a comprehensive understanding concerning dimensional changes in wood.

We can next calculate the Shannon entropy S from the results of the probability p_i ,

$$S = - \sum_{i=1}^N p_i \log p_i. \tag{6}$$

Figure 6 shows the variation of entropy S with β . The domain of β was set so that the entropy could be calculated. For both low and high-shrinkage samples, the earlywood images showed larger entropy S than the latewood images. Therefore, the low-shrinkage sample displayed a large entropy because of the high possession of earlywood. These results coincide with the optical micrographs (Fig. 1); specifically, the gradual transition from earlywood to latewood for low-shrinkage samples may be interpreted as a consequence of the distribution of the cell wall being more homogeneous. High-shrinkage samples show low entropy, where the distribution of the cell walls is a well-ordered repetitive pattern from earlywood to latewood. This can be explained from the distribution of brightness in the optical micrographs of the transverse section (Fig. 1). Figure 7 shows Histograms of the

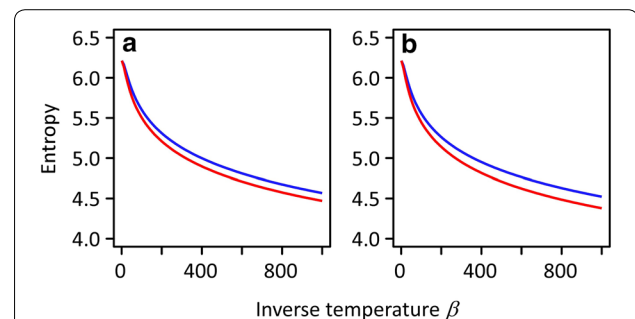


Fig. 6 Variation of the Shannon entropy with inverse temperature calculated from the spectra of the low-shrinkage sample (a) and high-shrinkage sample (b). Blue and red lines indicate earlywood and latewood images, respectively

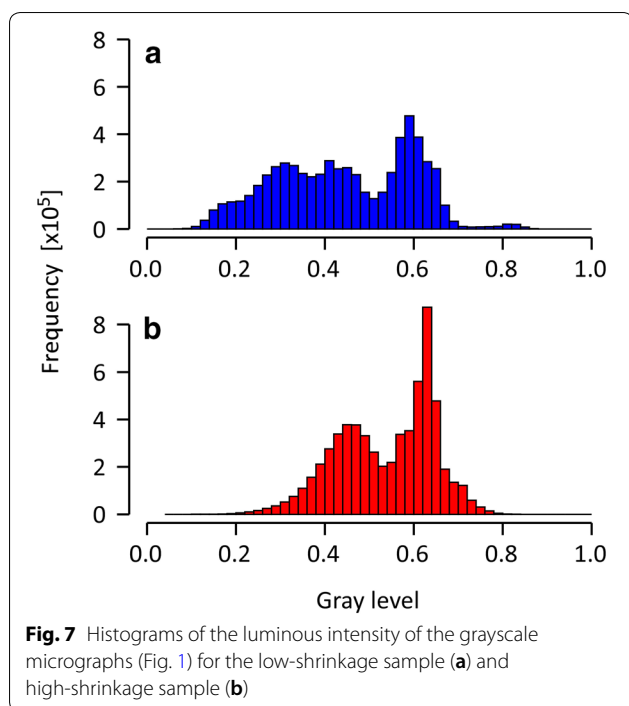


Fig. 7 Histograms of the luminous intensity of the grayscale micrographs (Fig. 1) for the low-shrinkage sample (a) and high-shrinkage sample (b)

luminous intensity of the grayscale micrographs for the low-shrinkage sample (a) and high-shrinkage sample (b). In general, the distribution of brightness shows the bimodality due to the contrast of cell walls and lumen. Sharpness of the peaks were obviously different between the samples. Two peaks were clearly identified in the micrographs of high-shrinkage sample but were spread in the low-shrinkage sample.

The physical approaches proposed in this study is suitable for evaluating phenomena where many factors contribute to a system cooperatively rather than individually [33–35]. As mentioned above, a wood may be regarded as a physical system with multiple degrees of freedom. Based on this suggestion, it seems that the spectral variables are like *generalized coordinates* in analytical mechanics [33]. That is, we consider the variation of data points as if they were the movements of a point particle in configuration space. Actually, in the Hamiltonian Monte Carlo method in simulating the posterior distribution, we consider the model parameter space of the probability distribution to be a configuration space and evaluate the potential energy using the logarithm posterior distribution [38]. Although the power spectra of image data were used in this study, the data from wood can be arbitrarily selected as long as they are multi-dimensional and spectral-like in this way of thinking. The proposed concept for considering the wood variation thus has very widely applicability.

Conclusions

Depending on the magnitude of the dimensional changes, obvious differences were found in the distribution patterns of cell walls in wood samples. The set of eigenvalues representing the energy states of the system can provide an evaluation of the distribution of cell walls in wood. The dimensional changes in wood are complex phenomena involving many factors. The approaches proposed is useful for evaluating phenomena in which many factors contribute to a system cooperatively rather than individually, and as it has no dependence on data type it has wide applicability. Because the idea is supported by universal theories of various physics fields, wood variations should be discussed from a more general perspective.

Acknowledgements

The authors deeply acknowledge Mr. Shogo Fukutomi and Ms. Asami Yoneda of Tottori University Forest for harvesting the sample trees. We thank Richard Haase, Ph.D, from Edanz Group (www.edanzediting.com/ac) for editing a draft of this manuscript.

Authors' contributions

HT performed all experiments and data analysis and was a major contributor in writing the manuscript. HH contributed to the preparation of sample materials and the data analysis. TF devised the overall concept of this study and contributed to discussion for the results. All authors read and approved the final manuscript.

Funding

No funding was received.

Availability of data and materials

Not applicable.

Competing interests

The authors declared no potential conflicts of interest with respect to the research, authorship, and/or publication of this article.

Author details

¹ Platform for Community-Based Research and Education (CoRE), Tottori University, Tottori 680-8553, Japan. ² Faculty of Agriculture, Tottori University, Tottori 680-8553, Japan.

Received: 7 May 2020 Accepted: 26 August 2020

Published online: 01 September 2020

References

- Panshin AJ, de Zeeuw C (1970) Textbook of wood technology, 3rd edn. McGraw-Hill, New York
- Schweingruber FH, Börner A, Schulze ED (2008) Atlas of woody plant stems. Evolution, structure, and environmental modifications. Springer, Berlin
- Dinwoodie JM (2000) Timber: its nature and behavior, 2nd edn. E & FN Spon Ltd, London
- Fujimoto T (2019) Evaluation of wood variation based on the eigenvalue distribution of near infrared spectral matrix. *J Near Infrared Spectrosc* 27:175–180
- Tsutsumi H, Haga H, Fujimoto T (2020) Variation in wood shrinkage evaluated by the eigenvalue distribution of the near infrared spectral matrix. *Vib Spectrosc*; Accepted 31th May 2020. <https://doi.org/10.1016/j.vibspec.2020.103091>.

6. Fujita M, Kaneko T, Hata S, Saiki H, Harada H (1986) Periodical analysis of wood structure I: some trials by the optical Fourier transformation. *Bull Kyoto Univ For* 60:276–284 **(in Japanese)**
7. Fujita M, Hata H, Saiki H (1991) Periodical analysis of wood structure IV: characteristics of the power spectral pattern of wood sections and application of non-microscopic wood pictures. *Mem Coll Agric Kyoto Univ* 138:11–23
8. Maekawa T, Fujita M, Saiki H (1993) Characterization of cell arrangement by polar coordinate analysis of power spectral patterns. *J Soc Mater Sci Jpn* 42:126–131 **(in Japanese)**
9. Fujita M, Midorikawa Y, Ishida Y (2002) Experimental conditions for quantitative image analysis of wood cell structure I: evaluation of various errors in ordinary accumulation image analysis. *Mokuzai Gakkaishi* 48:332–340 **(in Japanese)**
10. Ogata Y, Kadokawa T, Fujita M (2002) Experimental conditions for quantitative image analysis of wood cell structure II: nonmicroscopic image sampling over very wide areas using a film scanner. *Mokuzai Gakkaishi* 48:341–347 **(in Japanese)**
11. Kino M, Ishida Y, Doi M, Fujita M (2003) Experimental conditions for quantitative image analysis of wood cell structure III: precise measurements of wall thickness. *Mokuzai Gakkaishi* 50:1–9 **(in Japanese)**
12. Midorikawa Y, Fujita M (2003) Experimental conditions for quantitative image analysis of wood cell structure IV: general procedures of Fourier transform image analysis. *Mokuzai Gakkaishi* 50:73–82 **(in Japanese)**
13. Midorikawa Y, Ishida Y, Fujita M (2005) Transverse shape analysis of xylem ground tissues by Fourier transform image analysis I: trial for statistical expression of cell arrangements with fluctuation. *J Wood Sci* 51:201–208
14. Midorikawa Y, Fujita M (2005) Transverse shape analysis of xylem ground tissues by Fourier transform image analysis II: cell wall directions and reconstruction of cell shapes. *J Wood Sci* 51:209–217
15. Midorikawa Y, Fujita M (2005) Transverse shape analysis of xylem ground tissues by Fourier transform image analysis III: shape reconstruction of earlywood tracheids in 22 species and some parameters for normalizing cell shapes. *Mokuzai Gakkaishi* 51:218–226 **(in Japanese)**
16. Tu LW (2008) *An introduction to manifolds*. Springer Science + Business Media, LLC, New York
17. Tsuchikawa S (2007) A review of recent near infrared research for wood and paper. *Appl Spectrosc Rev* 42:43–71
18. Inagaki T, Ahmed B, Hartley ID, Tsuchikawa S, Reid M (2014) Simultaneous prediction of density and moisture content of wood by terahertz time domain spectroscopy. *J Infrared Milli Terahz Waves* 35:949–961
19. Santoni I, Callone E, Sandak A, Sandak J, Dirè S (2015) Solid state NMR and IR characterization of wood polymer structure in relation to tree provenance. *Carbohydr Polym* 117:710–721
20. Tsuchikawa S, Schwanninger M (2011) A review of recent near infrared research for wood and paper. Part 2. *Appl Spectrosc Rev* 48:560–587
21. Tsuchikawa S, Kobori H (2015) A review of recent application of near infrared spectroscopy to wood science and technology. *J Wood Sci* 61:213–220
22. Tsutsumi H, Oribe S, Haga H, Fujimoto T (2017) Nondestructive evaluation of wood properties in standing trees using vibrational spectra. *Mokuzai Gakkaishi* 63:291–296 **(in Japanese)**
23. Kabashima Y, Takahashi H (2012) First eigenvalue/eigenvector in sparse random symmetric matrices: influences of degree fluctuation. *J Phys A Math Theor* 45:325001
24. Mehta ML (2004) *Random matrices*, 3rd edn. Elsevier Ltd, London
25. Helrich CS (2009) *Modern thermodynamics with statistical mechanics*. Springer, Berlin
26. Landau DP, Binder K (2015) *A guide to Monte Carlo simulations in statistical physics*, 4th edn. Cambridge University Press, Cambridge
27. Tasaki H (2016) Typicality of thermal equilibrium and thermalization in isolated macroscopic quantum systems. *J Stat Phys* 163:937–997
28. Sekimoto K (2010) *Stochastic energetics*. Springer, Berlin
29. Cave ID (1972) A theory of the shrinkage of wood. *Wood Sci Technol* 6:284–292
30. Japanese Industrial Standards (1994) *Methods of test for woods*, JIS-Z-2101:1994. Japanese Industrial Standards, Tokyo
31. Barthelme S (2020) imager: Image Processing Library Based on 'Cimg'. R package version 1.3.3. <https://cran.r-project.org/web/packages/imager/imager.pdf>. Accessed 22 Aug 2020
32. Ligges U, Krey S, Mersmann O, Schnackenberg S (2018) tuneR: analysis of music and speech. R package version 1.3.3. <https://cran.r-project.org/web/packages/tuneR/tuneR.pdf>. Accessed 22 Aug 2020
33. Toda M, Kubo R, Saito N (1992) *Statistical physics I. Equilibrium statistical mechanics*, 2nd edn. Springer, Berlin
34. Kubo R, Toda M, Hashitsume N (1991) *Statistical physics II. Nonequilibrium statistical mechanics*, 2nd edn. Springer, Berlin
35. Schwabl F (2006) *Statistical mechanics*, 2nd edn. Springer, Berlin
36. Efron B, Tibshirani RJ (1993) *An introduction to the bootstrap*. Chapman and Hall, New York
37. Peng RD (2019) simpleboot: Simple Bootstrap Routines. R package version 1.1-7. <https://cran.r-project.org/web/packages/simpleboot/simpleboot.pdf>. Accessed 22 Aug 2020
38. Gelman A, Carlin JB, Stern HS, Dunson DB, Vehtari A, Rubin DB (2014) *Bayesian data analysis*, 3rd edn. CRC Press, Boca Raton, pp 351–467

Publisher's Note

Springer Nature remains neutral with regard to jurisdictional claims in published maps and institutional affiliations.

Submit your manuscript to a SpringerOpen® journal and benefit from:

- Convenient online submission
- Rigorous peer review
- Open access: articles freely available online
- High visibility within the field
- Retaining the copyright to your article

Submit your next manuscript at ► [springeropen.com](https://www.springeropen.com)